Int. J. Heat Mass Transfer. Vol. 30, No. 5, pp. 1017–1026, 1987
Printed in Great Britain

0017–9310/87 $3.00 + 0.00

Mass transfer of mixed gas flow crossing a high temperature graphite cylinder with chemical reactions and in-pore diffusion

M. OGAWA

Department of High Temperature Engineering, Japan Atomic Energy Research Institute, Tokai-mura, Ibaraki-ken 319-11, Japan

(*Received* 12 *June* 1986 *and in final form* 1 *October* 1986)

Abstract—An experimental study on mass transfer with chemical reactions and in-pore diffusion was performed in cross flow containing oxygen past a porous graphite cylinder placed in a high temperature environment. Reynolds numbers ranged from 533 to 2490, and cylinder temperatures ranged from 848 to 1120°C. It is concluded that chemical reactions do not significantly influence the mass transfer, and that the effect of in-pore diffusion on mass transfer can be estimated by using empirical relations for the corrosion rate and mass transfer.

1. INTRODUCTION

IN THE safety studies of high temperature gas-cooled reactors (HTGRs), a massive air ingress caused by a tube rupture in the primary circuit is regarded as a hypothetical event [1]. However, the corrosion of hot graphite materials by corrosive gases like oxygen mixed with helium gas during the massive air ingress into the reactor core may lead to the following consequences.

(1) Temperature rise of graphite materials used in fuels, reflectors and core support posts, caused by exothermic chemical reactions.

(2) Changes in external shape and internal pore of the graphite thus causing a reduction in mechanical strength.

(3) Disappearance of the graphite cladding material causing a release of fission products.

(4) Production of inflammable gases like carbon monoxide in the reactor containment.

Accordingly, it is necessary to investigate the corrosion process during the air ingress. The most important chemical reactions between oxygen and graphite are the heterogeneous reactions

$$C + xO_2 \rightarrow yCO + zCO_2 \quad (1)$$

$$C + CO_2 \rightleftarrows 2CO \quad (2)$$

and the homogeneous reaction

$$2CO + O_2 \rightarrow 2CO_2. \quad (3)$$

Since in general a reactive component transfers from one phase to another through the interface in heterogeneous reactions, a relation between the corrosion rate of a porous solid and the temperature of the solid reveals three characteristic regimes [2]. Figure 1 shows the relationship between the corrosion rate and the temperature, and the concentration of the corrosive gas distributed in the gas phase and the porous solid.

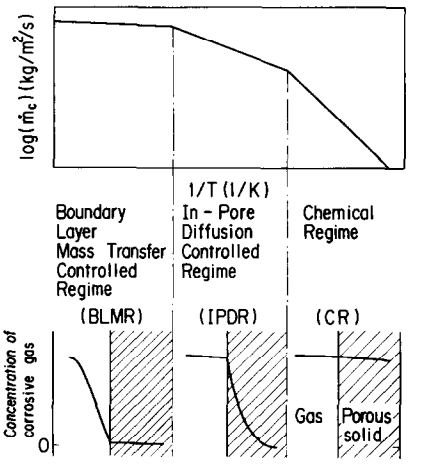

FIG. 1. Scheme of reactions between porous solid and corrosive gases.

In chemical reactions between graphite and oxygen, the three regimes are as follows:

Chemical regime (CR) at low temperature. The chemical reaction is so slow that the oxygen can penetrate the whole porous graphite with a small concentration gradient. The corrosion attack is fairly uniform in the graphite.

In-pore diffusion-controlled regime (IPDR) at medium temperature. The diffusion process of the oxygen in the pore becomes restrictive with regard to the corrosion rate. The oxygen concentration profile in the graphite becomes steeper with increasing temperature. The corrosion takes place at the surface and in an inside narrow zone near the surface. In the present experiment, the temperatures range from about 500 to about 900°C.

NOMENCLATURE

c_P	constant pressure specific heat
C	volume concentration
D	cylinder diameter before corrosion
f	C_{CO}/C_{CO_2}
h	characteristic length of test tube
k_s	mean diameter of particles
l	thickness of disk
m	mass
$\dot{m}$	mass flux, $\beta\rho(\omega_\infty - \omega_w)$
$\dot{m}_c$	corrosion rate
Δm	corroded mass
M	molar mass
Nu	Nusselt number, $\alpha D/\lambda$
P_{O_2}	partial pressure of oxygen gas
P_t	total pressure of gas mixture
Pr	Prandtl number, $c_P\mu/\lambda$
$\dot{q}$	heat flux, $\alpha(T_w - T_\infty)$
Q	volume flow rate
r	radius
r_{in}	inner radius of cylinder
Δr_{cor}	depth of corrosion attack
Re_D	Reynolds number, $UD\rho_{mix}/\mu_{mix}$
Sc	Schmidt number, $\mu/(\rho\delta)$
Sh	Sherwood number, $\beta D/\delta_{O_2/N_2}$
Δt	reacting time
T	temperature
U	bulk velocity in inner flow tube
V	volume
ΔV	corroded volume.

Greek symbols

α	heat transfer coefficient
β	mass transfer coefficient
δ	diffusion coefficient
θ	angle from stagnation point
$\Delta\theta$	angle interval
λ	thermal conductivity
μ	viscosity
ρ	density
ω	mass fraction.

Subscripts

b	bulk
c	cylinder
cal	calculated
cor	after corrosion
C	carbon
CO	carbon monoxide
CO_2	carbon dioxide
D	evaluated by cylinder diameter before corrosion
He	helium
m	mean
mix	gas mixture
ms	measured
N_2	nitrogen
O_2	oxygen
w	wall
θ	local
∞	free stream outside boundary layer
$\emptyset$	before corrosion.

Boundary layer diffusion-controlled regime (BLDR) at high temperature. Boundary layer diffusion is the dominant process to determine the corrosion rate. The corrosion attack is exclusively observed on the graphite surface. If the graphite is placed in a flow, the 'boundary layer mass transfer controlled regime (BLMR)' is a better expression because the mass transfer process includes the diffusion process in the boundary layer.

Especially, IPDR and BLMR are important for accident analyses in HTGRs because the corrosion rates in IPDR and BLMR are much larger than those in CR. The corrosion rate in IPDR has already been formulated as functions of the graphite temperature, the burnoff, and the oxygen partial pressure in other corrosion experiments [3, 4].

The corrosion rate in BLMR can be estimated by the relationship of the mass transfer on the assumption that the analogy between the mass transfer and the heat transfer is applicable to the problem. However, Specht and Jeschar [5] reported that the burnoff rate of burning carbon particles in a convective flow might be increased up to a factor of about two by the chemical reaction.

This is possibly explained as follows: oxygen in the boundary layer is consumed by the homogeneous reaction and the heterogeneous reaction. This heterogeneous reaction is the Boudouard reaction of chemical formula (2). These chemical reactions will lead to a steeper oxygen concentration gradient. An additional reason may be that the temperature distribution in the boundary layer has a pronounced maximum in the region of the homogeneous reaction, thus promoting mass transfer.

Mass transfer with chemical reactions is not yet well understood. The computer code REACT/THERMIX [6], which was developed for analyses of air and water ingress accidents in pebble bed HTGRs, must be certified by experiments. This code neglects the effect of chemical reactions on mass transfer. Furthermore, since mass transfer in an intermediate regime between IPDR and BLMR has not been well examined, it is necessary to study the effect of in-pore diffusion on mass transfer with chemical reactions.

Two graphite components in HTGRs, the fuel elements and the core support posts, might be significantly attacked by corrosion in BLMR. In the fuel elements, studies on the corrosion process in BLMR are in progress [7], but, there is little study of the core support posts.

The graphite cylinders of the core support posts in most designs of HTGRs are arranged in a triangular array. In an air ingress event of HTGR [8], the gas coolant flow containing oxygen intersects at right angles to the vertical circular cylinders in a high temperature environment. An experimental study on mass transfer in the presence of chemical reactions and in-pore diffusion is presented in this paper. The experiment [9] consists of an ascending crossflow containing approximately 5% oxygen which flows past one porous graphite cylinder placed in a high temperature environment.

2. EXPERIMENT

2.1. *Experimental facility*

A test section is shown in Fig. 2. A gas mixture of nitrogen and oxygen was heated in a preheater and then passed upward through flow tubes in a furnace. The gas mixture was released from a chimney to open air. A graphite circular cylinder was placed horizontally on top of the inner flow tube with an inner diameter of 290 mm and a height of 320 mm. The outer flow tube, which was concentric to the inner one, had an inner diameter of 350 mm and a height of 900 mm. Multi hole plates made the flow uniform and equalized the flow in the flow tube. The furnace had nine electric sheath heaters around the flow tubes.

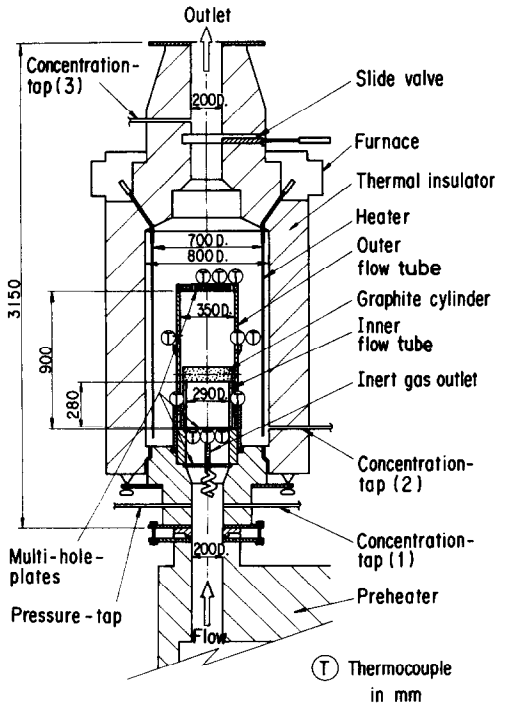

FIG. 2. Test section.

Figure 3 shows the graphite circular cylinder. It had a length of 320 mm, an inner diameter of 20 mm and an outer diameter of 100 mm. The inside hole was provided for easier measurement of the changes in shape due to corrosion. The outer diameter was designed to measure the change in shape with good accuracy and was of the same length as that of the core support post in PNP-500, which is designed as a prototype HTGR in Federal Republic of Germany. The graphite material, called V483T, was of nuclear grade. It had a nominal bulk density of 1780 kg m^{-3} and a porosity of 21.2%.

The furnace was equipped with one pressure tap at the inlet and with three concentration taps at the inlet, the test section and the outlet. Oxygen and carbon dioxide concentrations were measured by a mass spectrometer and carbon monoxide concentration was measured by a CO-analyzer.

Three thermocouples at the inlet and three at the outlet were used to measure gas temperatures. Six thermocouples were mounted on the wall of the flow tubes and treated with heat radiation shielding. The graphite cylinder temperatures were measured by seven thermocouples inserted into fine holes in the cylinder as shown in Fig. 3.

2.2. *Experimental procedures and conditions*

The mass and the dimensions of the cylinder were measured before the test. The bulk densities of the cylinders calculated by the measured mass and dimensions agreed with the nominal bulk density within $\pm 0.4\%$. A heat resistant material was plugged into the inside hole of the cylinder to protect this region from oxidation. The inner diameters of all cylinders remained the same after the test. The mass spectrometer and the CO-analyzer were calibrated before, periodically during, and after the test by using three kinds of standard gas mixtures of which the mixing ratios were known.

A large volume of nitrogen gas was blown through the preheater and the test section to eject oxygen before the tests. After an upper slide valve in the test section was partly closed, power was supplied to both the preheater and the furnace heater while nitrogen gas was flowing from an inert gas outlet (see Fig. 2) to prevent air from intruding into the preheater and the test section. When the temperatures rose to the desired level and became steady, oxygen gas was mixed into the nitrogen flow, and the total flow rate was regulated so that the oxygen volume concentration became approximately 5%.

The mass of the corroded cylinder was measured after each experimental run. Then, the cylinder was sliced into three disks (designated as Disk-1, -2 and -3 as shown in Fig. 3) with a thickness of 5 mm. The mass of each disk was measured to an accuracy of $\pm 1 \times 10^{-5}$ kg. The decreases in radius were measured circumferentially by a special slide gauge. The measurement errors of the radius and the decrease in

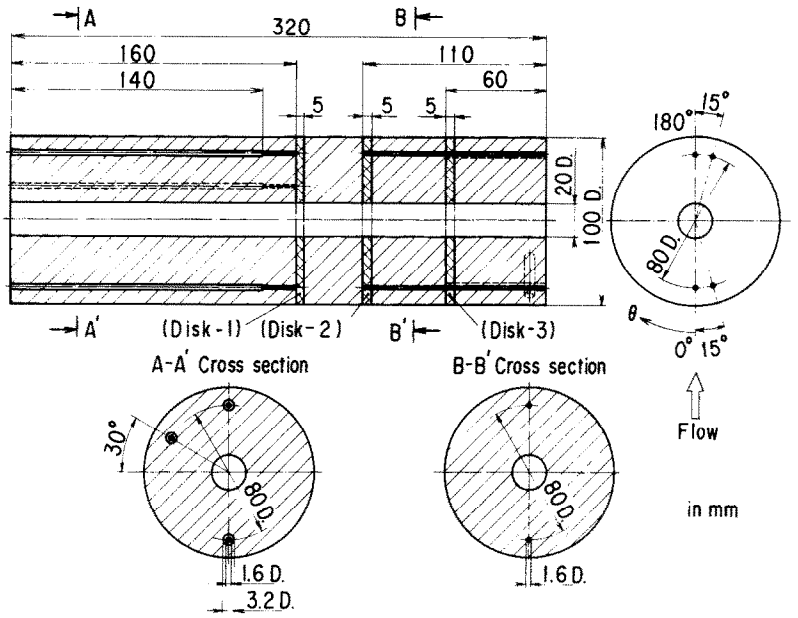

FIG. 3. Graphite cylinder.

Table 1. Experimental conditions

	Run number			
	1	2	3	4
Reynolds number	533	904	1660	2490
Oxygen concentration (%)	5.38	4.62	4.82	4.89
Gas pressure at test section $\times 10^5$(Pa)	1.013	0.989	1.019	1.023
Average gas temperature (°C)	1100	875	1030	823
Average cylinder temperature (°C)	1120	910	1070	848
Average wall temperature (°C)	1100	893	1040	822
Duration of corrosion experiment (h)	5.00	5.00	2.25	3.00

radius were within ± 0.02 and $\pm 0.2\%$ of each value, respectively.

Experimental conditions are listed in Table 1. Four test runs were made. The flow rates and the gas pressures were measured every other minute while adding oxygen, and these values were averaged. The temperature values were averaged after reaching the steady state because the temperature rose due to exothermic chemical reactions for several minutes after adding oxygen.

The experimental conditions of Runs 1 and 3 were in BLMR, and Runs 2 and 4 in the intermediate regime between BLMR and IPDR.

3. EXPERIMENTAL RESULTS AND DISCUSSION

3.1. *Changes in shape*

In a visual observation of the corroded surface of the cylinder, the appearance of the surface in Run 4 could be obviously distinguished from those in other runs. In detail, the surface of the cylinder in Run 4 was soft and was easily damaged. Graphite powder was attached to the lower part (near the stagnation point). The cylinders in other runs were hard enough not to be damaged.

Figure 4 shows longitudinal decreases of the radius of the cylinders. The abscissa is the longitudinal distance and the ordinate the decrease of radius measured from the original surface. The lower part of Fig. 4 shows the decreases of radius at the stagnation point and the upper part at an angle of 180° from the stagnation point. It was observed that these profiles were roughly symmetric with respect to the center of the flow tube. It is found that the distributions of the decreases of radius, which correspond to the velocity distribution of the flow, become more uniform with higher Reynolds number.

The circumferential distributions of the decreases of radius in Run 1 are shown in Fig. 5 as an example. The longitudinal decrease of radius shown in Fig. 4 was measured at the left half of the cylinder, and the circumferential one shown in Fig. 5 was measured at the other half. The measured points are smoothly connected by dotted lines. Although serious attention was given to the arrangement of the flow tubes and the cylinder to obtain a symmetric distribution of the decrease of radius, the distributions were asym-

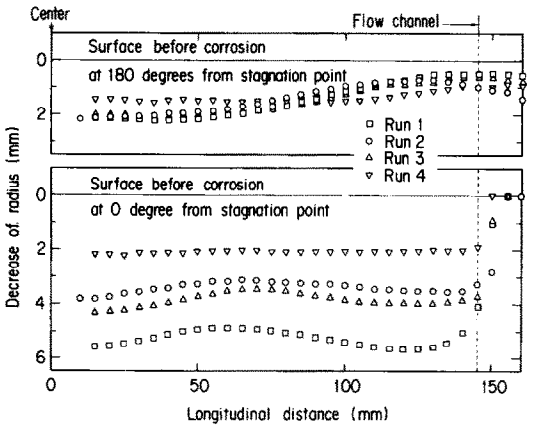

FIG. 4. Longitudinal deformation of the graphite cylinders at 0 and 180° from the stagnation point.

metrical in the present experiment. Near an angle of 180°, the decrease of radius of Disk-3 (near the end of the cylinder) differed from that of Disk-1 (at the center). This may be caused by the different flow pattern around the cylinder in the longitudinal direction because of the circular cross-section of the flow tube.

3.2. *Mean mass transfer coefficient*

The volume of the disk after the corrosion was calculated as follows:

$$V_{\mathrm{cor,cal}} = \sum_{i=1}^{n} \Delta V_{\mathrm{cor,cal},\theta_i} \tag{4}$$

$$= \sum_{i=1}^{n} \left(\int_{\theta_i-\Delta\theta/2}^{\theta_i+\Delta\theta/2} \int_{0}^{r} r\,\mathrm{d}r\,\mathrm{d}\theta - \Delta\theta r_{\mathrm{in}}^2/2 \right) l$$

where $\bar{r}$ of equation (4) was calculated from

$$\bar{r} = \int_{\theta_i-\Delta\theta/2}^{\theta_i+\Delta\theta/2} r^+\,\mathrm{d}\theta \Big/ \int_{\theta_i-\Delta\theta/2}^{\theta_i+\Delta\theta/2} \mathrm{d}\theta = r_i + a\Delta\theta^2/12 \tag{5}$$

where r^+ was approximated by a quadratic form of θ with the measured radii of r_{i-1}, r_i, r_{i+1} at angles of θ_{i-1}, θ_i, θ_{i+1}, respectively: $r^+ = a\theta^2 + b\theta + c$.

In the volume calculations of the corroded disks, the angle interval of 5, 10 or 15° had little influence on the absolute value of the volume. Therefore the angle interval of 5° was adopted for Disk-1 to draw a more detailed distribution of local mass transfer coefficients, and 10° for Disks-2 and -3.

The mass of the disk after the corrosion

$$m_{\mathrm{cor,cal}} = V_{\mathrm{cor,cal}}\rho_{\mathrm{b},\phi} \tag{6}$$

and the corroded mass of the graphite

$$\Delta m_{\mathrm{cor,cal}} = V_{\phi}\rho_{\mathrm{b},\phi} - m_{\mathrm{cor,cal}} \tag{7}$$

were calculated. The corroded mass of the graphite can also be obtained directly from the measured value

$$\Delta m_{\mathrm{cor,ms}} = V_{\phi}\rho_{\mathrm{b},\phi} - m_{\mathrm{cor,ms}}. \tag{8}$$

The difference between $\Delta m_{\mathrm{cor,cal}}$ and $\Delta m_{\mathrm{cor,ms}}$ indicates that the combustion of the graphite took place inside the cylinder by oxygen diffused into the pore. To estimate the degree of in-pore corrosion, the depth of the corrosion attack Δr_{cor} is defined by

$$\Delta r_{\mathrm{cor}} = (\Delta m_{\mathrm{cor,ms}} - \Delta m_{\mathrm{cor,cal}})/(2r_{\mathrm{av}}\bar{\rho}\pi l) \tag{9}$$

where $r_{\mathrm{av}} = [V_{\mathrm{cor,cal}}/(\pi l) + r_{\mathrm{in}}^2]^{1/2}$ and $\bar{\rho} = \rho_{\mathrm{b},\phi}/2$. The measurement errors of $(\Delta m_{\mathrm{cor,ms}} - \Delta m_{\mathrm{cor,cal}})$ in equation (9) were within ±20%. It is found [3, 4] that the depth of the corrosion attack decreases with increasing cylinder temperature in IPDR. However, the depth did not depend upon the temperature as shown in Table 2. This discrepancy might be partially explained by increasing surface corrosion with increasing flow rate. The inside corrosion attack of the cylinder was not remarkably affected by in-pore diffusion under the present experimental conditions.

The concentrations of carbon monoxide, carbon dioxide and oxygen measured at the outlet of the test section agreed well with those calculated from the corroded mass of the graphite in a mass balance calculation.

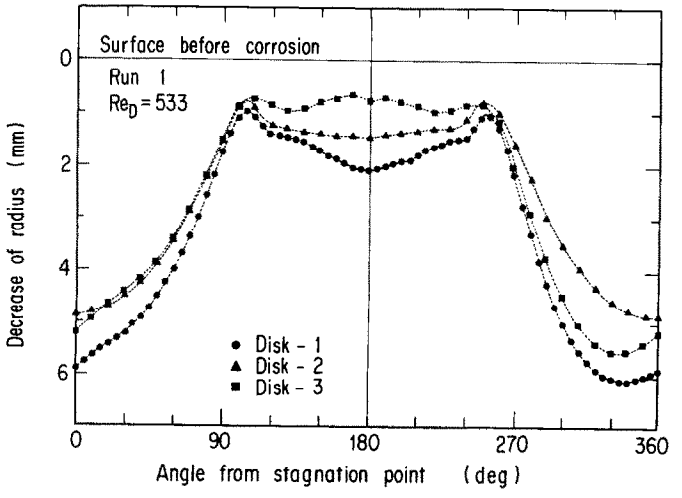

FIG. 5. Circumferential changes in shape of the corroded cylinders of Run 1.

Table 2. Depth of corrosion attack inside the graphite

		Run number 1	2	3	4
Average cylinder temperature (°C)		1120	910	1070	848
Reynolds number		533	904	1660	2490
Δr_{cor} (mm)	Disk-1	0.12	0.09	0.09	0.08
	Disk-2	0.12	0.06	0.06	0.21
	Disk-3	0.16	0.11	0.10	0.12
	Average	0.13	0.09	0.08	0.13

Reynolds and Sherwood numbers were evaluated from

$$Re_D = \frac{U\rho_{mix}D}{\mu_{mix}} \tag{10}$$

$$Sh = \frac{\beta D}{\delta_{O_2/N_2}}. \tag{11}$$

Although there are several definitions of the equivalent diameter, the diameter before the corrosion was used in the present study. If the changes in shape do not significantly influence the mass transfer, this definition is valid.

The film temperature and the pressure at the test section were used to calculate the thermal properties of a gas mixture with PRIAMUS computer code [10]. Since the gas volumes produced and destroyed by the chemical reactions were small, the components of the gas mixture were regarded as nitrogen and oxygen only, and the concentrations of nitrogen and oxygen at the inlet of the test section were used for the mixing ratio.

The mean mass transfer coefficients were defined as follows:

$$\beta_m = \frac{\dot{m}_{O_2}}{\rho_{mix}(\omega_{O_2,\infty} - \omega_{O_2,w})} \tag{12}$$

$$\dot{m}_{O_2} = \dot{m}_C \frac{M_{O_2}}{M_C}\frac{2+f}{2+2f} \tag{13}$$

$$\omega_{O_2,\infty} = \left(\frac{P_{O_2,\infty}}{P_t}\right)\frac{M_{O_2}/M_{N_2}}{1-(1-M_{O_2}/M_{N_2})(P_{O_2,\infty}/P_t)} \tag{14}$$

$$\omega_{O_2,w} = \left(\frac{P_{O_2,w}}{P_t}\right)\frac{M_{O_2}/M_{N_2}}{1-(1-M_{O_2}/M_{N_2})(P_{O_2,w}/P_t)} \tag{15}$$

$$\dot{m}_C = \frac{\Delta m_{cor,cal}}{\Delta t D\pi l} \tag{16}$$

where f is the concentration ratio of CO and CO_2 in chemical formula (1) and is given in ref. [4]. In the temperature range of about 850–1300°C the reaction of chemical formula (1) is dominant over all the others. In equations (14) and (15), the gases were assumed to be ideal. In equation (14), the partial pressure of oxygen in the free stream was calculated from the oxygen concentration at the inlet. In equation (15), the partial pressure of oxygen on the cylinder wall was defined to be equal to zero.

Since $\Delta m_{cor,ms}$ of equation (8) included the mass corroded inside the graphite and it is very difficult to measure circumferentially the local corroded mass $\Delta m_{cor,ms,\theta_i}$ to evaluate local mass transfer coefficients, $\Delta m_{cor,cal}$ of equation (7) was used.

The relationship between the mean Sherwood number and the Reynolds number is shown in Fig. 6. The sign in Fig. 6 stands for the average mean Sherwood number of the three disks, the maximum, and the minimum. The solid line represents the following equation:

$$Sh_m = 0.689 Re_D^{0.466} Sc^{1/3}. \tag{17}$$

Equation (17) is derived by the following manner: Hilpert [11] reported mean Nusselt numbers around a circular cylinder in air crossflow in his experiment

$$Nu_m = 0.615 Re_D^{0.466} \quad (40 \leqslant Re_D \leqslant 4000). \tag{18}$$

In consideration of the fact that the heat transfer coefficients are empirically proportional to the one-third power of the Prandtl number, equation (18) can be rewritten by using a Prandtl number of 0.71 for air

$$Nu_m = 0.689 Re_D^{0.466} Pr^{1/3}. \tag{19}$$

Since the Lewis number ($=Sc/Pr$) was about 0.95 nearly equal to 1 in the present experiment, if the analogy between the heat transfer and the mass transfer applies, equation (17) can be obtained directly from equation (19).

If chemical reactions have no effect on the mass transfer, the equation for the heat flux becomes similar

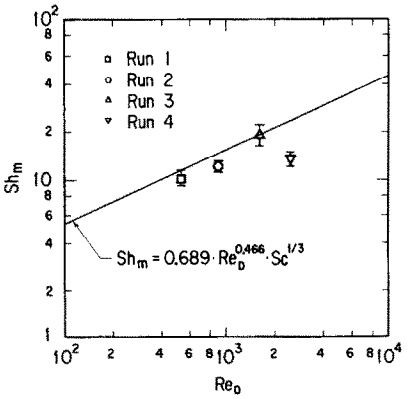

FIG. 6. Relationship between mean Sherwood numbers and Reynolds numbers.

to that for the mass flux for $\omega_w \ll 1$ as follows:

$$\dot{q} = -\left(\frac{\partial T}{\partial y}\right)_w \lambda \tag{20}$$

$$\dot{m} = \frac{-1}{1-\omega_w}\left(\frac{\partial \omega}{\partial y}\right)_w \delta\rho_{mix}. \tag{21}$$

Then, if either the heat transfer result or the mass transfer result is known, the result can be applied to the other transfer process [12]. Since the mass fraction of $\omega_{O_2,\infty}$ in the present experiment was less than about 0.06, $\omega_{O_2,w}$ was less than $\omega_{O_2,\infty}$, especially in BLMR where it was nearly equal to zero. So, the application of the analogy is taken as valid if chemical reactions have no effect.

Although the graphite powder was attached to the surface of the cylinder in Run 4, Nikuradse's roughness parameter $D/(2k_s)$ [13] was so large that the results of the mass transfer can be assumed to be for a smooth surface.

The diameter ratio of the cylinder to the flow tube D/h was 0.34 in the present experiment. This ratio may have some influence on the mass transfer. Only a small amount of data are available on the influence of the ratio. For crossflow around a circular cylinder, Eckert's experiments [14] examined D/h values of 0.11, 0.22 and 0.32 and Schmidt's experiments [15] included $D/h = 0.08$, 0.17 and 0.42. They neglected to consider this influence.

However, their results for large D/h values agreed with experimental results for uniform crossflows reported by Hilpert [11], for $D/h = 0.158$ by Krall and Eckert [16], and for $D/h = 0.072$ by van Meel [17]. Thus it is possible to compare the present results for $D/h = 0.36$ with the results of Hilpert [11], Eckert and Soehngen [14], and Krall and Eckert [16].

Experimental results of Runs 1 and 3 agreed fairly well with equation (17) in Fig. 6. Accordingly, the chemical reaction of formula (1) does not significantly influence the mean mass transfer coefficients. In addition, it is found that the diameter before the corrosion can be used as the equivalent diameter for small changes in shape, less than 6% of the diameter in the present experiment. The mean Sherwood numbers of Runs 2 and 4, especially Run 4, were smaller than those of equation (17). This implies the effect of in-pore diffusion.

3.3. *Local mass transfer coefficient*

Local corroded mass

$$\Delta m_{cor,cal,\theta_i} = [\Delta\theta V_\phi/(2\pi) - V_{cor,cal,\theta_i}]\rho_{b,\phi} \tag{22}$$

was calculated, and instead of $\dot{m}_c$ in equation (16), local mass flux

$$\dot{m}_{C,\theta_i} = \frac{2\Delta m_{cor,cal,\theta_i}}{\Delta\theta D\Delta t l} \tag{23}$$

was substituted into equation (13). Local mass transfer coefficients were obtained by the same evaluations of equations (11)–(15) as those in the mean mass transfer coefficient.

Circumferential distributions of the local mass transfer coefficients are shown in Figs. 7(a)–(d). Curved lines connect smoothly with the experimental values. The local Sherwood number becomes maximum at the stagnation point and minimum at the separation point of 85–120° from the stagnation point as observed in other experiments on the local heat transfer coefficient.

In Run 3 the minimum Sherwood number is observed again at a point downstream from the separation point as shown in Fig. 7(c). This is because a region similar to the separation region appears between the eddy region and the secondary eddy region, as was seen in the visualization experiment made by Nagata *et al.* [18].

In IPDR, the corrosion rate depends upon the cylinder temperature, the oxygen partial pressure, and the burnoff [4]. If an experimental condition of IPDR is set in the present experimental facility, since the distributions of the temperature are expected to be fairly uniform circumferentially, the local corrosion rate, that is, local Sherwood number will become uniform. The circumferential distribution of the local Sherwood numbers in Run 4 was fairly uniform in spite of the highest Reynolds number among the present experimental conditions. This suggests the importance of the effect of in-pore diffusion on the mass transfer in the surface and in the boundary layer.

Figure 8 shows a comparison of the present local mass transfer coefficients with the local heat transfer coefficients in other experiments [14, 16]. The local Sherwood and Nusselt numbers were normalized by the mean Sherwood number of equation (17) and the mean Nusselt number of equation (19), respectively. The agreement between both results was fairly good, especially at the stagnation point. It is thought that a little difference between both results near the point of 180° from the stagnation point is caused by the flow expanding from the inner flow tube to the outer flow tube.

As a result of Runs 1 and 3, it is concluded that the chemical reactions do not significantly influence the local mass transfer coefficient.

3.4. *In-pore diffusion*

Dependence of the corrosion rate on the cylinder temperature is shown in Fig. 9. Broken lines indicate the corrosion rates of BLMR calculated by equations (11)–(15) and (17) in which the oxygen concentration at the inlet of the test section is used for $P_{O_2,\infty}$ and $P_{O_2,w}$ is made equal to zero. Dash one dotted lines are calculated by the following equation obtained in another IPDR experiment [4] for graphite material A3-3 placed in a helium gas flow:

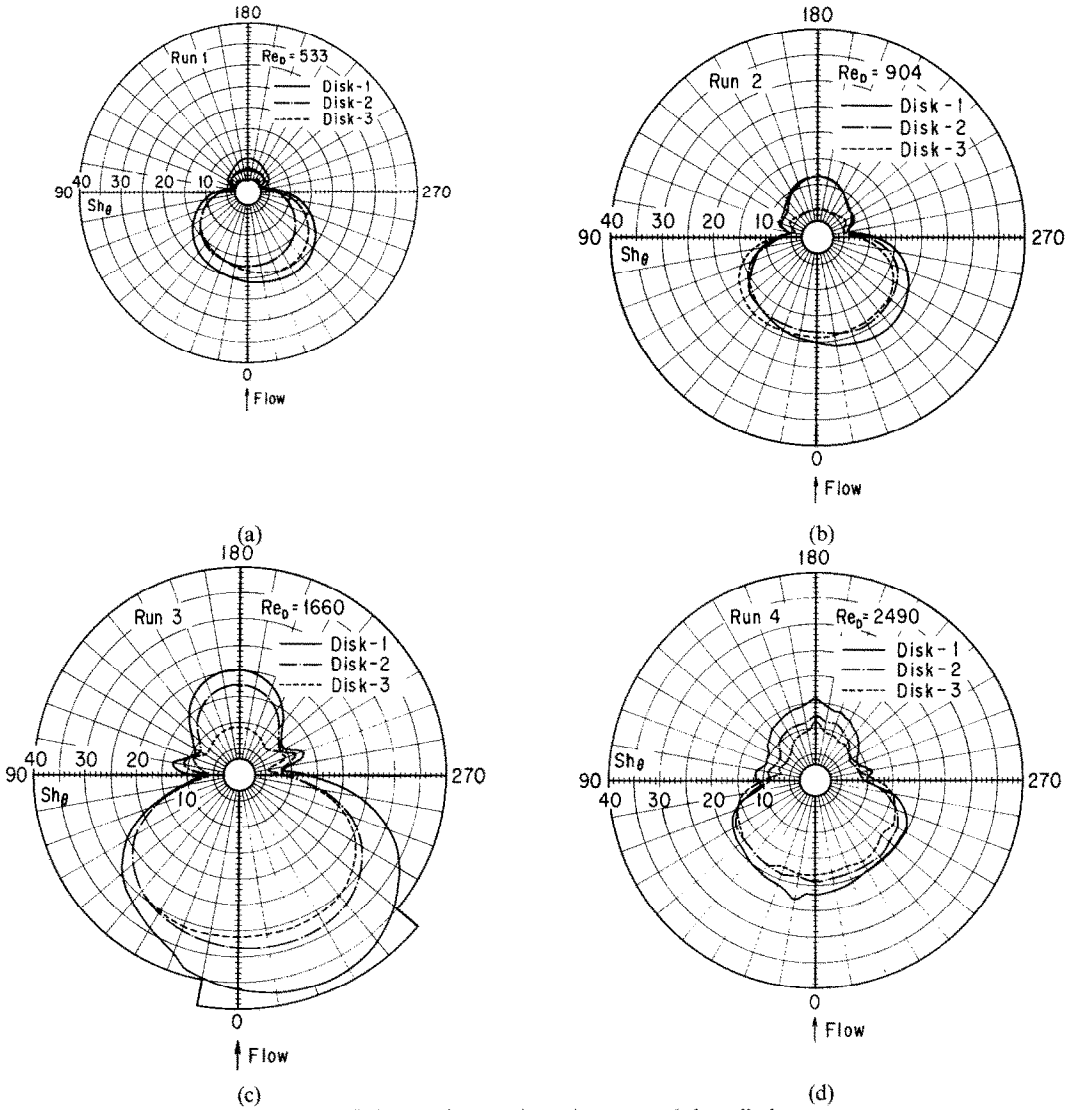

FIG. 7(a–d). Local Sherwood numbers around the cylinders.

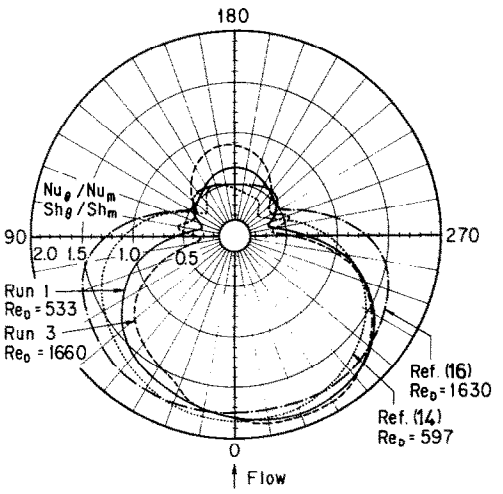

FIG. 8. Comparison of the present local Sherwood numbers with local Nusselt numbers of others.

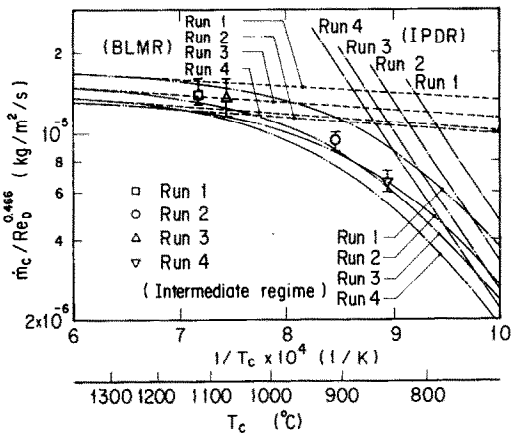

FIG. 9. Corrosion rates in BLMR and intermediate regime.

$$\dot{m}_C = \frac{2.34\times10^{-2}\exp(-12{,}850/T)P_{O_2,w}}{1+0.0039\exp(1569/T)(P_{O_2,w})^{1/2}} \times \left(\frac{\delta_{O_2/N_2}}{\delta_{O_2/He}}\right)^{0.5} T_\phi \quad (24)$$

where $P_{O_2,w}$ is made equal to the oxygen concentration. The last term in parentheses on the right-hand side of equation (24) represents the factor modifying the difference of the operating gas. The corrosion rate for the graphite material V483T was only slightly different from that of equation (24), as demonstrated in another experiment [19].

The partial pressure of oxygen gas on the wall $P_{O_2,w}$ is determined from $\dot{m}_C^{BLMR} = \dot{m}_C^{IPDR}$ ($\dot{m}_C^{BLMR}$ is calculated from equation (17) and equations (11)–(15) and $\dot{m}_C^{IPDR}$ from equation (24)), and the corrosion rate in the intermediate regime is obtained as drawn by dash two dotted lines of Fig. 9. The corrosion rates of Runs 1 and 3 agreed fairly well with those of BLMR, and the corrosion rates of Runs 2 and 4 agreed well with those of the intermediate regime.

From these results of the corrosion rates, it is verified that the effect of the in-pore diffusion on the mean mass transfer coefficient is estimated by the empirical relations of the corrosion rate of equation (24) and the mean Sherwood number of equation (17). The dominance of the in-pore diffusion effect in Run 4 explains the more uniform distribution of the local Sherwood numbers for that run as shown in Fig. 7(d).

4. CONCLUDING REMARKS

An experimental study on the mass transfer has been carried out in mixed gas flow crossing a porous graphite cylinder placed in a high temperature environment in the presence of chemical reactions and in-pore diffusion of oxygen. The main conclusions can be summarized as follows:

(1) In BLMR, the mean Sherwood numbers obtained in the present experiment agreed fairly well with the empirical relation of the mass transfer of equation (17) on the basis of the analogy between heat transfer and mass transfer. Also, the local Sherwood numbers agreed with the results of the local Nusselt numbers by others.

(2) The chemical reactions of chemical formulas (1)–(3) did not have a significant influence on the mass transfer under the present experimental conditions. In the REACT/THERMIX code, it is unnecessary to account for the chemical reactions under HTGR air ingress accident conditions.

(3) The corrosion rates of the intermediate regime between IPDR and BLMR were verified to be estimated from the empirical relations of the corrosion rate and the mean mass transfer coefficient.

Acknowledgements—The author wants to express his gratitude to Dr J. Fassbender of Kernforschungsanlage Jülich GmbH (KFA Jülich) for his continuous encouragement and support of the present study. He also is obliged to Prof. E. Achenbach, Dr W. Katscher, Dr R. Moormann and Mr B. Stauch of KFA Jülich for valuable discussions and support. He is grateful to Mr H. K. Hinssen and Mr H. Seeboth for their assistance in carrying out the experiment and their valuable comments and guidance in the data reduction.

REFERENCES

1. R. Moormann and R. Finken, Graphitkorrosionsuntersuchungen zu massiven Lufteinbruchstörfällen mit primärem Sauerstoffeintritt in die Säulenhalle am Beispiel des HTR-PNP-500, *Proc. Jahrestagung Kerntechnik*, Berlin, pp. 203–206 (1983).
2. M. Rossberg and E. Wicke, Transportvorgänge und Oberflächenreactionen bei der Verbrennung graphitischen Kohlenstoffs, *Chemie-Ingr-Tech.* **28,** 181–185 (1956).
3. W. Katscher, H. K. Hinssen, R. Moormann, W. Delle and E. Wallura, Changes in the macroporosity of nuclear reactor graphite under oxygen corrosion, *High Temperature—High Pressure* **13,** 275–279 (1981).
4. H. K. Hinssen, W. Katscher and R. Moormann, Kinetik der Graphit/Sauerstoff-Reaktion im Porendiffusionsbereich (Teil 1: Matrixmaterialien A3-3 und A3-27), Jül-1875 (Nov. 1983).
5. E. Specht and R. Jeschar, Kopplung von Konvection mit chemischer Kinetik beim Abbrand von Kohlepartikeln, *Ber. Bunsenges. Phys. Chem.* **87,** 1095–1099 (1983).
6. R. Moormann and K. Petersen, REACT/THERMIX—Ein Computercode zur Berechnung der störfallbedingten Graphitkorrosion in Kugelhaufenreaktoren, Jül-1782 (Apr. 1982).
7. B. Stauch, SUPERNOVA, ein Experiment zur Untersuchung der Graphitkorrosion bei schweren Luft- und Wassereinbruchstörfällen in Kugelhaufen-HTR, KFA-ISF-IB-3/84 (July 1984).
8. R. Moormann, Effect on delays in afterheat removal on consequences of massive air ingress accidents in High-Temperature Gas Cooled Reactors, *J. Nucl. Sci. Tech.* **21,** 824–835 (1984).
9. M. Ogawa, B. Stauch, R. Moormann and W. Katscher, An experimental investigation on mass transfer in presence of chemical reactions on a graphite cylinder in crossflow, Jül-Spez-336 (Nov. 1985).
10. R. Finken and R. Moormann, PRIAMUS—Ein Rechenprogramm zur Bestimmung thermopysikalischer Stoffwerte von Gasmischungen aus O_2, N_2, CO, CO_2, He, H_2O, H_2, und CH_4, Jül-1916 (May 1984).
11. R. Hilpert, Wärmeabgabe von geheizten Drähten und Rohren im Luftstrom, *Forsch. Geb. IngWes.* **4,** 215–224 (1933).
12. E. R. G. Eckert and R. M. Drake, Jr., *Analysis of Heat and Mass Transfer*, p. 170. McGraw-Hill, New York (1972).
13. W. M. Kays and M. E. Crawford, *Convective Heat and Mass Transfer*, p. 185. McGraw-Hill, New York (1980).
14. E. R. G. Eckert and E. Soehngen, Distribution of heat transfer coefficients around circular cylinders in crossflow at Reynolds numbers from 20 to 500, *Trans. Am. Soc. Mech. Engrs* **74,** 343–347 (1952).
15. E. Schmidt and K. Wenner, Wärmeabgabe über den Umfang eines angeblasenen geheizten Zylinders, *Forch. Geb. IngWes.* **12,** 65–73 (1941).
16. K. M. Krall and E. R. G. Eckert, Local heat transfer around a cylinder at low Reynolds number, *Trans. Am. Soc. Mech. Engrs*, Series C, *J. Heat Transfer* **95,** 273–275 (1973).
17. D. A. van Meel, A method for the determination of local convective heat transfer from a cylinder placed normal to an air stream, *Int. J. Heat Mass Transfer* **5,** 715–722 (1962).

18. H. Nagata, H. Funada, K. Kawai and T. Matsui, Unsteady flows in the vortex region behind a circular cylinder started impulsively (1st report, feeding mechanism of vorticity and onset of turbulence) (in Japanese), *Trans. Japan Soc. Mech. Engrs*, Series B **51**, 738–747 (1985).
19. H. K. Hinssen, Private communication.

TRANSFER DE MASSE D'UN DEBIT DE GAZ MELANGES TRAVERSANT UN CYLINDRE EN GRAPHITE A HAUTE TEMPERATURE AVEC REACTIONS CHIMIQUES ET DIFFUSION EN PORE

Résumé—Une étude expérimentale sur transfer de masse avec réactions chimiques et diffusion en pore a été effectuée au moyen d'un débit contenant gaz d'oxygéne qui traverse un cylindre poreux en graphite mis dans un environnement à haute température. Les nombres de Reynolds se situent entre 533 et 2490 et les températures de cylindre entre 848 et 1120°C. On a conclu que les réactions chimiques n'a pas d'influences significatives sur le transfer de masse et que l'on peut esitmer l'effet de diffusion en pore sur le transfer de masse sur la base des relations empiriques entre facteur de corrosion et transfer de masse.

MASSENÜBERGANG VON MISCHGASFLUß ÜBER EINEN GRAPHITZYLINDER HOHER TEMPERATUR MIT CHEMISCHEN REAKTIONEN UND DIFFUSION IN DEN POREN

Zusammenfassung—Es wurde eine experimentelle Studie über den Massenübergang mit chemischen Reaktionen und Diffusion in den Poren für den Querfluß von Sauerstoff enthaltendem Gas über einen porösen Graphitzylinder in einer Umgebung mit hoher Temperatur durchgeführt. Die Reynoldschen Zahlen lagen im Bereich von 533 bis 2490, und die Zylindertemperaturen lagen im Bereich von 848 bis 1120°C, und die Zylindertemperaturen lagen im Bereich von 848 bis 1120°C. Es wurde geschlossen, daß die chemischen Reaktionen den Massenübergang nicht wesentlich beeinflussen und daß die Wirkung der Diffusion in den Poren auf den Massenübergang durch den empirischen Zusammenhang zwischen der Korrosionsrate und dem Massenübergang geschätzt werden kann.

МАССОПЕРЕНОС СМЕШАННОГО ПОТОКА ГАЗА, ОБТЕКАЮЩЕГО ВЫСОКОНАГРЕТЫЙ ГРАФИТОВЫЙ ЦИЛИНДР, ПРИ ХИМИЧЕСКИХ РЕАКЦИЯХ И ВНУТРИПОРОВОЙ ДИФФУЗИИ

Аннотация—Проведены эксперименты по изучению массопереноса при химических реакциях и внутрипоровой диффузии в поперечном потоке, содержащем кислород и обтекающем графитовый цилиндр, помещенный в среду с высокой температурой. Числа Рейнольдса изменялись в диапазоне от 533 до 2490, температура цилиндра—от 848 до 1120°C. Найдено, что химические реакции не оказывают существенного влияния на массоперенос, а роль внутрипоровой диффузии может быть оценена с помощью эмпирических зависимостей для скорости коррозии и массопереноса.